Secular variation of Earth's gravitational harmonic J_2 coefficient from Lageos and nontidal acceleration of Earth rotation

C. F. Yoder, J. G. Williams & J. O. Dickey

Jet Propulsion Laboratory, California Institute of Technology, Pasadena, California 91109, USA

B. E. Schutz, R. J. Eanes & B. D. Tapley

Center for Space Research, University of Texas at Austin, Austin, Texas 78712, USA

Analysis of $5\frac{1}{2}$ years of Lageos satellite range data reveal significant residual nodal signatures: an acceleration and annual and semiannual periods. These signatures primarily reflect variations in the zonal gravitational harmonic J_2 coefficient and hence the polar moment of inertia. The implied decrease of $\dot{J}_2 = -3 \times 10^{-11}$ yr^{-1} is consistent with both historical observations of the nontidal acceleration of the Earth's rotation and models of viscous rebound of the solid Earth from the decrease in load due to the last deglaciation.

ARTIFICIAL Earth satellites have been used since the dawn of the space age to determine the Earth's permanent gravity field. This field is normally represented as a series of spherical harmonic functions with constant coefficients[1]. The zonal harmonics of degree l are designated J_l, and the J_2 coefficient is directly related to the Earth's oblateness. Within the past decade, a special class of satellites (Geos, Starlette, and most recently, Lageos) has been used to determine, in addition to the permanent gravity field, the amplitude and phase of the semidiurnal and diurnal tidal variations in the Earth's nonzonal gravity field[2,3]. A decade ago Kozai[4], Paddock[5] and Wagner[6] attempted to use artificial satellites to measure either seasonal (Kozai) or secular (Paddock, Wagner) changes in the gravity field. However, the tracking accuracy necessary to detect these small variations was not then available. More recently, Bender and Goad[7] and Gaposchkin[8] have discussed or used Lageos' data to detect the seasonal and tidal ($\leq$1 yr) variations caused by similar signatures in J_2.

We show here that Lageos' orbit (particularly its node, Ω) is sensitive to secular (and periodic) changes in J_l, especially $\dot{J}_2$. The $\dot{J}_2$ derived from the observed secular acceleration $\ddot{\Omega}$ is consistent with the nontidal acceleration of the Earth's rotation[9]. The $\dot{J}_l$ expected from viscous rebound following the last great deglaciation[10,11] are examined, and this mechanism is shown to be a plausible explanation for the observed effects.

The passive satellites Lageos[12] and Starlette are particularly well suited for geodynamical studies as both are accurately ranged from the Earth using pulsed laser beams. Also, the design of these satellites was chosen to minimize the effects of air drag and light pressure. Their orbits lie well above the dense atmosphere and both have small cross-sectional area to mass ratio A/M. This ratio and the orbital parameters (semimajor axis a, eccentricity e, inclination I, orbital period P, periods of circulation of node $P(\Omega)$, and argument of pericentre (w), $P(w)$) are given in Table 1. Figure 1 describes the orientation of Lageos' orbit with respect to the Earth.

Lageos' node and Earth rotation

It has been assumed that the Lageos orbit would provide a stable benchmark for the determination of the nonlinear changes in the accumulated rotation angle of the Earth (effectively UT1) by measuring the orientation of the Earth with respect to Lageos' node Ω. This section demonstrates that both UT1 and Ω show proportional, similar sized responses to J_2 variations, so this view must be revised if these variations can be detected. When compared with a separate source of UT1 the Lageos tracking data provides the opportunity to detect J_2 variations and discriminate sources of UT1 variation which arise from J_2 changes from those which do not. Tidal deformation[13–15], seasonal changes in groundwater[16] and mean sea level and viscous rebound of northern Canada[17,18] after the last deglaciation are mechanisms which produce changes in UT1 in response to changes in J_2. A change in the Earth's volume in response to a change in the gravitational constant, thermal expansion of the oceans[19], exchange of angular momentum between atmosphere and mantle[20] or fluid core and mantle[21], and exchange of angular momentum via tidal torques with Sun and Moon are mechanisms for UT1 change which have small effect on J_2. Of these mechanisms only angular momentum exchange with the atmosphere and tidal deformations have been previously detected.

A satellite's node, argument of perigee w and mean anomaly l are primarily sensitive to variations in the even zonal harmonic

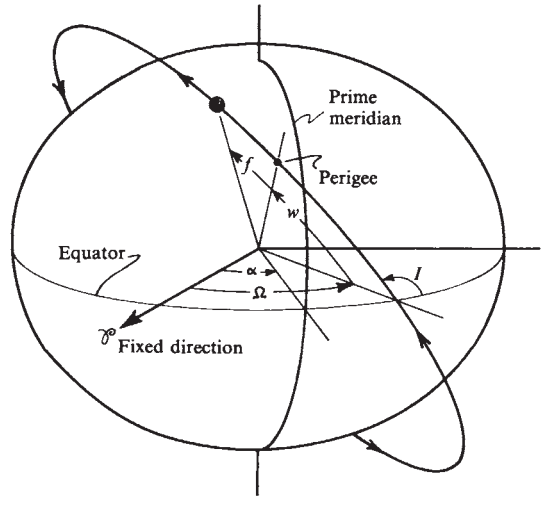

Fig. 1 Geometrical relationships and definitions: the angle α, which is nearly a linear function of UT1, measures the Earth's rotation with respect to a fixed direction, γ. The longitude of the ascending node, Ω, and the inclination, I, determine the orientation of the satellite's orbit plane. The argument of perigee, w, is measured in the orbit plane from the equator to the orbit's point of closest approach to the Earth.

0028-0836/83/260757—06$01.00

coefficients. The node may also be affected by unmodelled variations in inclination which would alter our estimates of the variation in J_l. The following dynamical equation[1]

$$\frac{\mathrm{d}}{\mathrm{d}t}\delta\Omega = -\tfrac{3}{2}n\left(\frac{R_e}{a}\right)^2 \frac{\cos I}{(1-e^2)^2}(\delta J_2 + \delta J_4 f_4 + \delta J_6 f_6 - \delta I \tan I J_2) \quad (1)$$

$$f_4 = \frac{5}{8}\left(\frac{R_e}{a}\right)^2 (7\sin^2 I - 4)\frac{(1+\frac{3}{2}e^2)}{(1-e^2)^2} \quad (2)$$

$$f_6 = \frac{35}{64}\left(\frac{R_e}{a}\right)^4 (8 - 36\sin^2 I + 33\sin^4 I)\frac{(1+5e^2+\frac{15}{8}e^4)}{(1-e^2)^4} \quad (3)$$

describes the perturbation in Ω caused by the variations δJ_2, δJ_4 and δJ_6 and δI. Here $n = 2\pi/P$ is the orbital mean motion and $R_e = 6{,}378$ km is the Earth's equatorial radius. For Lageos, the inclination factors $f_4 = 0.37$ and $f_6 = 0.08$ are sufficiently large that we must be concerned with the magnitude of δJ_4 and δJ_6 relative to δJ_2 predicted by various mechanisms. We shall argue later that the assumption that δJ_2 dominates in equation (1) is a reasonable first approximation.

The variations in w, l and Ω caused by δJ_2 are proportional. The approximate relations for small e are

$$\delta w(J_2) \simeq -\frac{(4 - 5\sin^2 I)}{2\cos I}\delta\Omega(J_2) \quad (4)$$

$$\delta l(J_2) \simeq -\frac{(2 + 3\sin^2 I)}{2\cos I}\delta\Omega(J_2) \quad (5)$$

In principle, all three parameters are sensitive to δJ_2, but the mean anomaly always suffers sizeable irregular variations caused by mechanisms such as variable air drag. For an elliptical orbit the perigee motion would be usable, but Lageos' orbit is nearly circular and the range measurement is sensitive to the product $e\delta w$. Thus, the node is the practical parameter to investigate for Lageos.

δJ_2 is directly proportional to the variation in the polar moment of inertia C for deformation mechanisms which preserve volume[22] such as tidal deformation and mass redistribution over the Earth's surface. The relationship between δJ_2 and δC for these mechanisms is

$$\delta J_2 = \frac{3\delta C}{2MR^2} \quad (6)$$

where R is the Earth's mean radius. Variations in Earth spin rate ω directly follow from the conserved angular momentum, $C\omega$.

$$\frac{\delta\omega(J_2)}{\omega} = -\delta J_2 \frac{2MR^2}{3C} \quad (7)$$

Denoting the variations in UT1 driven by δJ_2 as $\delta\mathrm{UT1}(J_2)$ [that is, integrated $\delta\omega(J_2)$], we find

$$\delta\Omega(J_2) = K\delta\mathrm{UT1}(J_2) \quad (8)$$

$$K = \frac{9}{4}\frac{C}{MR^2}\frac{n}{\omega}\left(\frac{R_e}{a}\right)^2 \cos I \quad (9)$$

The above formula applies only for a solid Earth, including oceans. A rotationally-decoupled mantle and fluid core slightly modify the constant of proportionality K (ref. 15). For Lageos, the appropriate K for equilibrium tidal deformations varies from -0.477 to -0.437 for a rotationally decoupled and coupled fluid core, respectively. The latter value is appropriate for slow secular changes in J_2. Lageos' node moves about 7 m arc s in response to a change in $\delta\mathrm{UT1}(J_2)$ of 1 ms of time (1 ms = 15 m arc s).

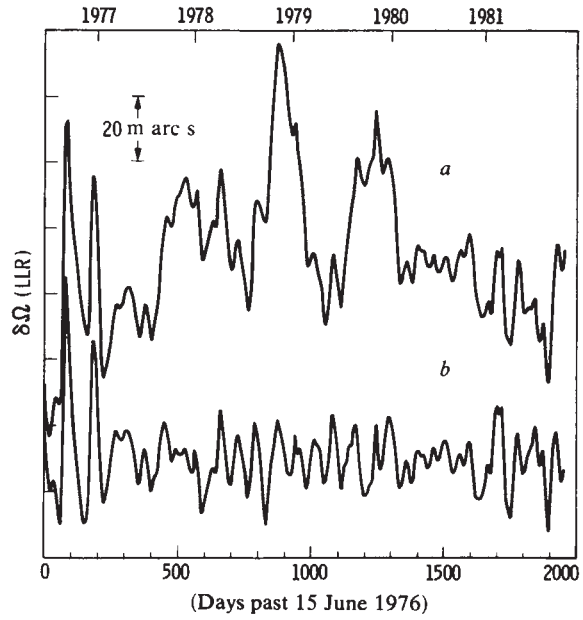

Fig. 2 Residual $\delta\Omega$(LLR) after removal of the five-frequency (a) and eight-frequency solution (b).

Data analysis

Fits of the Lageos tracking data to sophisticated dynamical models still leave residual signatures in the orbital parameters. Since signatures in the node and errors in the adopted UT1 are indistinguishable, two independent sources of UT1 were used in this analysis. Five nodal periodicities were associated with diurnal and semidiurnal tides on the Earth and correspond to small ocean-tide corrections to the nominal tidal model used.

Table 1 Orbital parameters

Satellite	Period (h)	a (km)	e	I (deg)	$P(\Omega)$ (days)	$P(\omega)$ (days)	A/M (cm^2 g^{-1})
Lageos	3.758	12,270	0.004	109.94	1046	−1707	0.0069
Starlette	1.735	7,330	0.020	49.8	−109	93	0.0096

Table 2 18.6 yr, annual and semiannual amplitudes (in m arc s): solution for Lageos' node compared with nominal tidal model and seasonal models

	$\sin\Omega_\leftmoon$	$\cos\Omega_\leftmoon$	$\sin\odot$	$\cos\odot$	$\sin 2\odot$	$\cos 2\odot$
$\delta\Omega$(LLR)	−96 ± 88	−151 ± 22	−13.8 ± 1.5	12.2 ± 2.0	−4.4 ± 1.5	−2.6 ± 1.5
$\delta\Omega$(BIH)	−68 ± 109	−177 ± 29	−11.5 ± 2.0	−3.1 ± 2.7	−3.7 ± 2.0	−1.1 ± 2.0
Nominal tidal model						
Ref. 15	1,160	0	11.0	−0.4	−32.4	−12.2
Nontidal seasonal model (δJ_2 only)						
Ref. 14			−1	24	−0.7	−2.5
Ref. 13			−17	21	0	−1.7

Solar angle $\odot = 0°$ on 1 January.

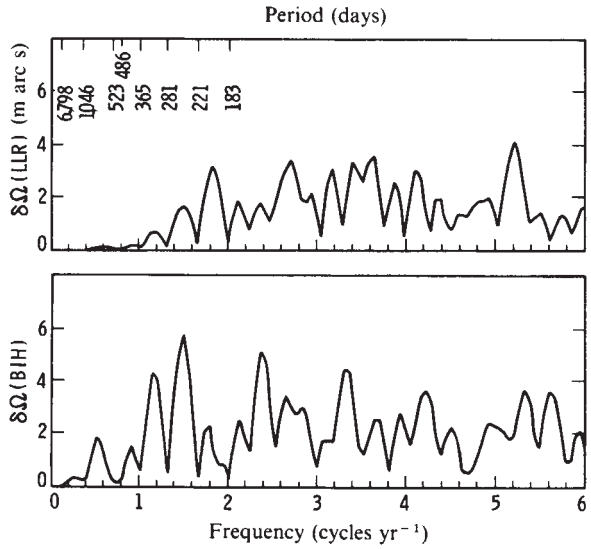

Fig. 3 Amplitude spectra for $\delta\Omega$(LLR) and $\delta\Omega$(BIH) after removal of the eight-frequency solution.

In addition annual and semiannual periodicities and a large acceleration were present in the node and these constitute the evidence for the J_2 variations that we are seeking.

Lageos laser ranges were analysed between May 1976 and December 1981. The model included forces from the irregular gravity field of the Earth, solar, lunar and planetary (Venus through Saturn) gravitational perturbations, drag, solar radiation pressure, and nominal tidal expressions[3]. The nominal amplitudes for 18.6, 1 and 1/2 yr tidal signatures, which have been removed from Ω, are given in Table 2. UT1 was modelled with Bureau International de l'Heure (BIH) circular D, 5-day smoothed values, but polar motion was solved for at the same intervals. After this $5\frac{1}{2}$ yr fit, the corrections to orbital elements were derived at 5–10 day intervals from the range residuals to display perturbations unrepresented in the model. Corrections to the 'node' really reflect corrections to Ω − UT1, while the errors in both the Ω measurement by Lageos and independent measurements of UT1 by other techniques are comparable in size. UT1 derived by the techniques of lunar laser ranging (LLR) and very long baseline interferometry (VLBI) have demonstrated submillisecond (of time) accuracies[23,24] and are expected to possess good long-term stability. Consequently a second set of node corrections was derived from the UT1 differences between one of these (LLR) and BIH. The smoothed node corrections are designated $\delta\Omega$(BIH) and $\delta\Omega$(LLR). The corrections will be used to infer the equivalent changes in the gravity field using the theoretical $\delta\Omega$ in equation (1).

Both the node corrections using BIH UT1 and the irregularly spaced UT1(LLR) − UT1(BIH) values had nonuniform uncertainties. These quantities, $y(t_j)$ with uncertainties σ_j, were smoothed and interpolated at 5-day intervals of time t using weighted gaussian smoothing.

$$Y(t) = s(t)^2 \sum_j [y(t_j)/\sigma_j^2] \exp[-(t-t_j)^2/2\tau^2] \qquad (10)$$

$$s(t)^{-2} = \sum_j (1/\sigma_j)^2 \exp[-(t-t_j)^2/2\tau^2] \qquad (11)$$

where $s(t)$ is an uncertainty associated with the smoothed quantity $Y(t)$. The sums were limited to ±35 days around t with a choice of $\tau = 10$ days (FWHM = 23.5 days). This filters out more than half of the amplitude for spectral periods shorter than ≈60 days while for UT1 (BIH) the half amplitude point is reached at ≈100 days. The smoothed tabulations of UT1(LLR) − UT1(BIH) were subtracted from $\delta\Omega$(BIH) to get $\delta\Omega$(LLR), the error in the latter being taken from the quadratic sum of the other two errors.

Spectra of $\delta\Omega$(BIH) and $\delta\Omega$(LLR) showed that tidal corrections to the nominal ocean model were necessary. Consequently we solved for empirical corrections (two components each) due to the (nonzonal) diurnal and semidiurnal ocean tides which cause orbital perturbations at periods of 1045.6, 522.9, 485.5, 280.7, and 221.3 days. A straight line was included to absorb a constant J_2 uncertainty. The residuals from the five-frequency (12-parameter) weighted least squares fit to $\delta\Omega$(LLR) are shown as Fig. 2*a*. In addition to the obvious curvature, there is a sizeable annual and a detectable semiannual term which we interpret as originating from J_2 variations. Eight-frequency (18-parameter) solutions included 1/2-, 1-, and 18.61-yr periods. The amplitudes are given in Table 2 with the nominal zonal tides which were originally removed. The post-fit residuals for $\delta\Omega$(LLR) are displayed in Fig. 2*b*. The curvature and seasonal signatures have been removed. The two peaks near the beginning of the data span have low weight. They match a stretch of sparse Lageos' data and a gap in the LLR measurements. The weighted post-fit r.m.s. residuals for $\delta\Omega$ are 10 and 7.7 m arc s using the BIH and LLR UT1 respectively. We had to accept the restriction that the $5\frac{1}{2}$ yr data span does not permit separating quadratic and 18.6 yr (Ω_ℓ) terms, though physical causes exist for both. At the middle of the data span the 18.6-yr terms yield accelerations of

$$\delta\ddot{\Omega}(\text{LLR}) = -14.7 \pm 1.3 \quad \text{m arc s yr}^{-2} \qquad (12)$$

and

$$\delta\ddot{\Omega}(\text{BIH}) = -18.2 \pm 1.6 \quad \text{m arc s yr}^{-2} \qquad (13)$$

The amplitude spectra of the residuals from the eight-frequency fits are shown in Fig. 3. It is evident that the low-frequency components of the residuals are reduced when the LLR values of UT1 are used. This is in accord with the spectra of UT1(LLR) − UT1(BIH), which decrease from low to high frequency as shown by Fliegel *et al.*[23]. The high-frequency end of the spectra also appears to be improved using UT1(LLR). This suggests that the Lageos and LLR data are detecting real variations in UT1 at 60–90 day periods. These frequencies have largely been filtered out of UT1(BIH). We do not know the cause of the peak at 70.2 day, but note that it is 1/8 the circulation period of Lageos' node relative to the Sun. In generating the $1-\sigma$ uncertainties of Table 2, we have taken a noise level of 2.0 and 1.5 m arc s from the spectra of $\delta\Omega$(BIH) and $\delta\Omega$(LLR), respectively. The post-fit, r.m.s. residuals can be adjusted for the noise absorbed during the fits to conclude that the real weighted r.m.s. differences are respectively 12 and 9 m arc s when BIH and LLR values of UT1 are used.

The inclination residuals have also been fit with the five nonzonal tidal frequencies. The earliest data show a negative bias in the residuals. If a linear trend is included in the fit then $\delta\dot{I} = 1.9 \pm 0.7$ m arc s yr^{-1}, equivalent to a positive $\ddot{\Omega}$ of 11.5 m arc s yr^{-2}. We suspect incomplete separation of inclination and polar motion with the earlier, less accurate data. If we remove the first year of data, $\delta\dot{I}$ is reduced to 0.1 ± 0.3 m arc s yr^{-1} and is insignificant. However, the shorter data set results in only modest changes in $\delta\ddot{\Omega}$ (for example, $\delta\ddot{\Omega}$(LLR) = −14.3 ± 2.4 m arc s yr^{-2}).

Rubincam[37] reports a substantially smaller value for the secular acceleration ($\delta\ddot{\Omega} = -10.8 \pm 2.3$ m arc s yr^{-2}) based on an independent analysis of Lageos' ranges. The source of the apparent conflict is not yet understood.

Tidal dissipation and $\ddot{\Omega}$

The lunar node Ω_ℓ passes through 168.7° at the midpoint of the data span. The very significant $\cos\Omega_\ell$ correction term mimics a term proportional to the square of the time t. Physical mechanisms for both signatures exist.

By far the largest zonal tide variation in Lageos' node (see nominal values in Table 2) or UT1 is the 18.6-yr tide associated with the precession of the lunar node, but most of this tide was originally removed with the nominal model. A $\cos\Omega_\ell$ term would arise from a phase shift of the nominal, tidally driven

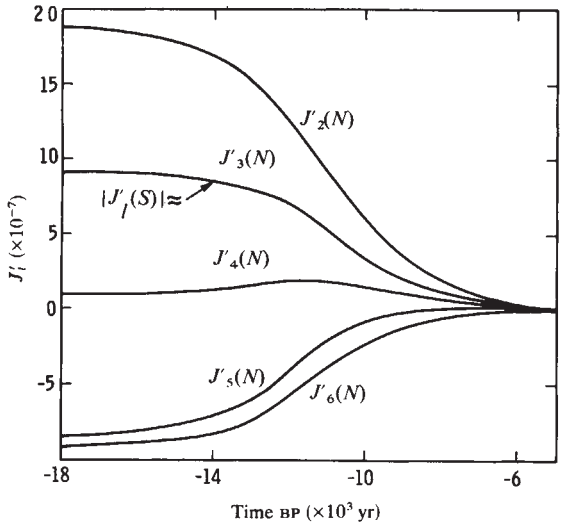

Fig. 4 Elastically compensated load coefficients $J'_l(N)$ and $J'_l(S)$ associated with melting history of Laurentide–Fenoscandia and Antarctic ice sheets, respectively.

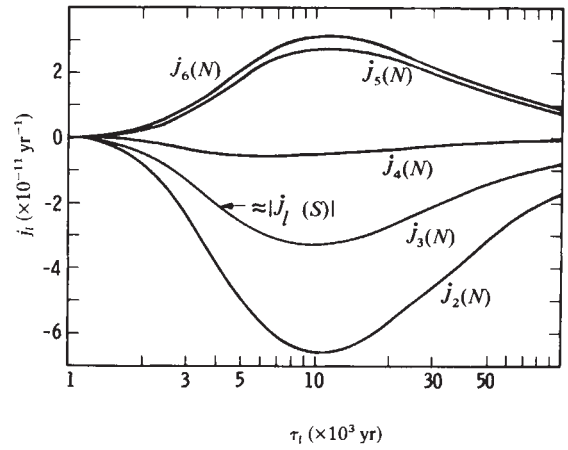

Fig. 5 Present $\dot{J}_l(N)$ and $\dot{J}_l(S)$ as function of τ_l based on melting history and equation (18).

sin Ω_ℓ term and this phase shift depends on dissipation by solid body friction or ocean currents. Dissipation causes a time delay T in the tidal variation of δJ_2. If T were about 0.4 yr or the dissipation factor $Q \simeq |1/\dot{\Omega}_\ell T| \simeq 8$, then tidal dissipation could account for the entire signature. The ocean tides contribute 12% of the amplitude of the nominal zonal tide model, but they are both the major uncertainty in tidal calculations and the expected source of any significant dissipation since the mantle Q is probably >100. Even if the oceanic Q were near unity, it would only account for about half of the observed cos Ω_ℓ signature. Such large oceanic dissipation is usually deemed unlikely based on Proudman's[25] estimate of dissipation by bottom friction. Physical measurements of the amplitude and phase of the 18.6-yr ocean tide height are highly uncertain[26–28], but indicate large phase shifts from equilibrium at different tide gauge stations. However, Rossiter[27] finds that the mean phase is near zero. He also finds that the mean amplitude of the 18.6-yr ocean tide is depressed by a factor of 2/3 while Currie[28] finds that the amplitude is near its equilibrium value. By elimination we conclude that most of the curvature seen in Lageos' node is a secular acceleration with only a small, unknown part related to dissipation in the 18.6-yr tidal constituent. The driving J_2 variation is thus dominantly a rate of change of nontidal origin.

Deglaciation and $\dot{J}_l$

Earth has experienced several ice ages which recur on a 10^5-yr time scale. 20,000 yr ago, massive ice sheets up to 3 km in thickness covered much of northern Canada and Scandinavia with a total mass $\approx 3\times10^{22}$ g equivalent to an 80-m change in sea level. At the the same time, the Antarctic ice sheet was considerably thicker than at present[32,33]. Several investigators[10,11] have suggested that the Earth's gravity field still possesses memory of the last melting episode which ended about 5,000 yr ago. Also, deglaciation may be responsible for the $\approx$2 m arc s yr^{-1} secular polar motion as well as the nontidal acceleration of ω (refs 11, 17, 18). This section demonstrates that the rate of change of J_2 is compatible with the glacial rebound hypothesis and predicts a nontidal acceleration of Earth rotation in reasonable accord with historical values.

With the observed acceleration in equations (12) and (13) for the two UT1 sources, we derive from equation (1) secular changes in J_2 of

$$\dot{J}_2(\text{LLR}) = (-3.5 \pm 0.3)\times10^{-11} \quad \text{yr}^{-1} \tag{14}$$

$$\dot{J}_2(\text{BIH}) = (-4.4 \pm 0.4)\times10^{-11} \quad \text{yr}^{-1} \tag{15}$$

Equations (1), (14), and (15) predict the following nontidal acceleration in Earth rotation, $(\dot{\omega}/\omega)_{\text{NT}}$.

$$(\dot{\omega}/\omega)_{\text{NT}}(\text{LLR}) = 7.1 \pm 0.6\times10^{-11} \quad \text{yr}^{-1} \tag{16}$$

$$(\dot{\omega}/\omega)_{\text{NT}}(\text{BIH}) = 8.8 \pm 0.8\times10^{-11} \quad \text{yr}^{-1} \tag{17}$$

Both are in agreement with Morrison and Stephenson's[9] determination $(\dot{\omega}/\omega)_{\text{NT}} = 8.4 \pm 1.3\times10^{-11}$ yr^{-1}) using Babylonian lunar eclipse timings. Their estimate is sensitive to the adopted values for the lunar tidal acceleration $\dot{n}_\ell$ (ref. 29) and the contribution of the solar tide to the tidal $\dot{\omega}$. Their value for the Earth's nontidal acceleration (really a $\approx$25-century average) is reduced to $(\dot{\omega}/\omega)_{\text{NT}} = 6.3 \pm 0.9\times10^{-11}$ yr^{-1} using improved estimates for $\dot{n}_\ell$ from LLR[30] ($\dot{n}_\ell = -2.52 \pm 0.12$ m arc s yr^{-2}) and the Earth's tidal acceleration: $(\dot{\omega}/\omega)_{\text{T}} = -26.4 \pm 1.4\times10^{-11}$ yr^{-1}. We can also improve these estimates of $(\dot{\omega}/\omega)_{\text{NT}}$ in equations (16) and (17) by correcting in equation (1) for the secular $\dot{J}_4$ and $\dot{J}_6$ changes predicted by the rebound hypothesis.

The viscous response of the solid Earth to this changing surface load is approximately described by the following relaxation equation

$$\left(\frac{\mathrm{d}}{\mathrm{d}t} + \frac{1}{\tau_l}\right) J_l = -\frac{\mathrm{d}}{\mathrm{d}t}(J'_l(N) + J'_l(S)) \tag{18}$$

where $J'_l(N)$ and $J'_l(S)$ refer to the elastically compensated load coefficients associated with the Fenoscandian–Laurentide and Antarctic ice sheets, respectively. The complexities of rigid lithosphere and fluid core are serious complications which are missing from this simple equation, but these effects are not expected to change the final result by >30%.

The time history of the $J'_l(N)$ coefficients shown in Fig. 4 were derived from Wu and Peltier's[31] Ice-2 maps which describe the recession of the northern ice caps from 18,000 to 4,000 yr BP. The time history of the Antarctic sheet is less certain[32]. From Hughes *et al.*[32,33] map of the excess ice covering Antarctica 18,000 yr ago, we find that the initial $J'_l(S) \approx (-1)^l 9\times10^{-7}$. If the melting of the northern and southern ice caps proceeds at the same rate, then we find that $J'_l(S) \approx (-1)^l J'_l(N)$ to within 20%. From Fig. 4, we can deduce that $J'_2(S) \approx J'_2(N)/2$, $J'_4(S) \gg J'_4(N)$ while the $l=3$ and $l=6$ contributions tend to cancel.

The present values of $\dot{J}_l(N)$ and $\dot{J}_l(S)$ as a function of the relaxation time τ_l are shown in Fig. 5. For $\dot{J}_2 = -3.5\times10^{-11}$ yr^{-1}, the allowed τ_2 are 3,100 or 65,000 yr which correspond to mantle viscosities of 4×10^{22} P or 8×10^{23} P, respectively[11]. The remaining τ_l probably do not differ from τ_2 by more than a factor of two. Peltier[34] estimates that $\tau_5 \approx 2{,}500$ yr from the history of raised beaches in Hudson Bay.

If all τ_l are equal, then the values of τ_2 and $\dot{J}_2$ which account for Lageos' secular acceleration (12) is slightly changed to

$$\tau_2 = 2{,}800 \quad \text{yr}; \qquad \dot{J}_2 = -3.1\times10^{-11} \quad \text{yr}^{-1} \tag{19}$$

$$\tau_2 = 75{,}000 \quad \text{yr}; \qquad \dot{J}_2 = -3.2\times10^{-11} \quad \text{yr}^{-1} \tag{20}$$

The change is primarily due to the contribution to $\ddot{\Omega}$(LLR) from $\dot{J}_4$ since $\dot{J}_6$ is apparently small. Both $\dot{J}_2$ predict $(\dot{\omega}/\omega)_{NT} \simeq 6\times10^{-11}\,\text{yr}^{-1}$, in close agreement with the revised determination of Morrison and Stephenson[9].

However, there are other considerations which affect the smaller τ_2 solution. The relaxation hypothesis also predicts that $(\dot{\omega}/\omega)_{NT}$ is not constant but decreases exponentially with time constant τ_2. We would expect that the present $(\dot{\omega}/\omega)_{NT} \lesssim 4\times10^{-11}\,\text{yr}^{-1}$ using $\tau_2 \lesssim 3{,}000$ yr and the 25-century average for $(\omega/\omega)_{NT}$. The least-squares fit of post 1650 observations[29] suggest that the present $(\dot{\omega}/\omega)_{NT} \simeq 17\times10^{-11}\,\text{yr}^{-1}$. The discrepancy between the 3- and 25-century averages for $(\dot{\omega}/\omega)_{NT}$ is usually attributed to quasi-periodic exchanges of angular momentum between fluid core and mantle. Further analysis of the relaxation mechanism will be required to determine if there is a serious conflict between the historical $(\dot{\omega}/\omega)_{NT}$ and the $(\dot{\omega}(J_2)/\omega)_{NT}$ from Lageos with a 'small' τ_2.

Seasonal variations in Ω

Comparison of the observed seasonal corrections with the nominal tidal coefficients of Table 2 indicates that the corrections are too large to attribute to errors in ocean tide models. The cause of the corrections is primarily nontidal J_2 variations (δJ_2 (annual) $\simeq 3\times10^{-10}$ and δJ_2 (semiannual) $\simeq 1\times10^{-10}$). The equivalent annual and semiannual amplitudes in δUT1(J_2) are about 2.6 and 0.7 ms respectively. Each represents ~10% of the total seasonal variations in UT1 at those periods.

We are only partly successful in reconciling the observed annual and semiannual amplitudes in $\delta\Omega$ given in Table 2 with independent calculations of the nontidal seasonal contributions to δJ_2 and Earth rotation. The primary sources of nontidal seasonal δJ_2 are variations in groundwater, sea level and air mass. Table 2 also displays the predicted amplitudes based on the compilations of Munk and MacDonald[13] and Lambeck[14]. Lambeck's estimate should be more accurate as he uses improved estimates of the groundwater variation[16]. There is a ≈45° phase difference between the annual $\delta\Omega$(LLR) solution and Lambeck's prediction. Part of this discrepancy may be that the δJ_4 and δJ_6 contributions have been omitted from the model calculation. However, if these seasonal variations are primarily controlled by changes in mean sea level (a debatable point), then the expected scaling of the J_l is roughly[35]; $\delta J_2 \simeq -2\delta J_3 \simeq 3\delta J_4 \simeq -\delta J_5 \simeq 4\delta J_6$, and δJ_2 clearly dominates.

In any case we have demonstrated that Lageos' orbit is sensitive to seasonal changes in the gravity field. We should also mention that the seasonal δJ_2 are expected to be noisy, varying in amplitude and phase from year to year and displaying spectral amplitude at all frequencies. How much of this seasonal 'noise' contributes to the residual amplitude in the $\delta\Omega(LLR)$ spectra would be pure conjecture at present.

Future prospects

Our ability to separate the 18.6-yr and t^2 signatures should rapidly improve with time. Table 3 shows the expected uncertainties if we attempt to solve simultaneously for a sin Ω_ℓ, cos Ω_ℓ, and a quadratic polynomial in t as the data span is increased. These estimates assume that the background spectral amplitude noise is ~1.5 m arc s. At least $1\frac{1}{2}$ more years of data are required before the attempted separation of the long periodic and secular accelerations of Ω is justified, and as much as five additional years may be needed to obtain a strong separation.

Table 3 Estimated uncertainties as function of data span

Data span (yr)	sin Ω_ℓ (m arc s)	cos Ω_ℓ (m arc s)	(t^2 yr^{-2}) (m arc s)
$5\frac{1}{2}$	±300	±1,400	±80
7	90	160	10
8	60	80	5
10	30	20	1.7
12	20	10	1.1

Meanwhile, confirmation of our results may be possible from an independent analysis of the Starlette orbit. Starlette, launched on 1 February, 1975 (14 months before Lageos) is considerably more sensitive to variations in δJ_2: $\delta\Omega(J_2) \simeq 5\,\delta\text{UT1}(J_2)$. Also the inclination parameter $f_4 = 0.04$ for Starlette is small enough to allow separation of δJ_2 and δJ_4 if δJ_6 is small. The major reservation is that Starlette's orbit is much more difficult to model numerically. Presently, the r.m.s. residuals to a fit of 1 yr of Starlette data is ≈8 m compared with Lageos r.m.s. residuals of ≈2 m for $5\frac{1}{2}$ yr of data[3].

Future improvements in the Lageos modelling may permit detection of seasonal and secular variations in the odd zonal J_l. In this case, the orbital eccentricity e and argument of perigee w are the orbital parameters most sensitive to changes in J_3, J_5, and so on. The dynamical equation appropriate to a high I, small e orbit is best described using the complex variable $p = e\exp(-iw)$ where $i = \sqrt{-1}$.

$$\frac{dp}{dt} + i\dot{w}_0 p \simeq \frac{3}{2} n \sin I \left(\frac{R_e}{a}\right)^3 (\delta J_3 f_3 + \delta J_5 f_5) \tag{21}$$

$$f_3 = 1 - \tfrac{5}{4}\sin^2 I \tag{22}$$

$$f_5 = -\frac{5}{32}\left(\frac{R_e}{a}\right)^2 (8 - 28\sin^2 I + 35\sin^4 I) \tag{23}$$

$$\dot{w}_0 \simeq 3\left(\frac{R_e}{a}\right)^2 n J_2 f_3 \tag{24}$$

The inclination parameters equal $f_3 = -0.11$ and $f_5 = -0.45$ for Lageos while $\dot{w}_0 \simeq -2\pi/1{,}707$ days. The viscous rebound hypothesis predicts that $\dot{J}_3 \simeq -1\times10^{-12}\,\text{yr}^{-1}$ and $\dot{J}_5 \simeq 1\times10^{-11}\,\text{yr}^{-1}$ for $\tau_3 \simeq \tau_5 \simeq 2{,}500$ yr. Therefore, the expected drift rate for p is 2 m arc s yr^{-1}. The seasonal δJ_5 may also dominate in equation (21). A plausible annual $\delta J_5 \simeq 2\times10^{-10}$ in amplitude, will produce a 9 m arc s annual variation in p. Both of these signatures should be detectable from the present data record. The major reservation here is that variable drag forces[36] and seasonal and irregular variations in the Earth light pressure force may produce similar signatures and are not yet adequately modelled. An improved model for the light pressure force is being developed.

Conclusion

We have demonstrated that Lageos' node is sensitive to seasonal and secular changes in the Earth's gravity field, especially $\dot{J}_2$. The observed secular acceleration $\delta\ddot{\Omega}(\text{LLR}) = -14.7 \pm 1.3$ m arc s yr^{-2} can be driven by a secular change in J_2 of $-3\times10^{-11}\,\text{yr}^{-1}$. This value for $\dot{J}_2$ includes corrections from $\dot{J}_4$ and $\dot{J}_6$ predicted by mantle relaxation following deglaciation [Fig. 4 and equation (18)], for a mantle viscosity near 3×10^{22} P. Any dissipation in the 18.6-yr tide will reduce the derived $\dot{J}_2$ further. This $\dot{J}_2$ predicts a modern value for the nontidal acceleration of the Earth's rotation $(\dot{\omega}/\omega)_{NT} \simeq 6\times10^{-11}\,\text{yr}^{-1}$. An independent analysis of Starlette's orbit might confirm this prediction for $\dot{J}_2$.

Annual and semiannual signatures in Ω have been detected and agree in amplitude, but not in phase with independent estimates of the contributions to δJ_2 and Earth rotation from changes in groundwater, sea level and air mass. There must be improvements in the seasonal model before we say that this discrepancy is significant. The inferred UT1 (δJ_2) variations are ~10% of the known seasonal terms.

In the future, it should be possible to detect similar variations in the odd J_l from their effect on Lageos' eccentricity. With five more years of Lageos' data, we should also be able to detect the effects of dissipation on the 18.6-yr ocean tide if the $Q(18.6\,\text{yr}) \lesssim 50$.

Finally, we have indirectly demonstrated that UT1(LLR) has better long term stability (spectral period ≥ 60 days) than does UT1(BIH) from a comparison of the post-fit amplitude

spectrum of the residual $\delta\Omega$ using both sources of UT1. While Lageos may determine short-period variations in UT1 well, at longer times scales its unique sensitivity to changes in the zonal harmonics will be more valuable than its direct sensitivity to UT1 since this permits isolation of the component of UT1 variations caused by J_2 changes.

We thank W. R. Peltier for supplying maps of the Ice-2 model. In this research, C.Y., J.W. and J.D. were supported by Jet Propulsion Laboratory, California Institute of Technology, under contract NAS7-918. The University of Texas at Austin group (B.S., R.E. and B.T.) were supported under NASA contract NAS5-25991.

Received 24 January; accepted 5 May 1983.

1. Kaula, W. M. *Theory of Satellite Geodesy* (Blaisdell, Waltham, 1966).
2. Cazenave, A. & Daillet, S. *J. geophys. Res.* **86,** 1659–1663 (1981).
3. Eanes, R., Schutz, B. & Tapley, B. in *Proc. 9th int. Symp. on Earth Tides*, (ed. Kuo, J. T.) (E. Schweiterbart'sche Verlagsbuchhandlung, in the press).
4. Kozai, Y. *Spec. Rep. 236* (Smithsonian Astrophysical Observatory, Cambridge, Massachusetts, 1970).
5. Paddock, S. J. *J. geophys. Res.* **72,** 5760–5762 (1967).
6. Wagner, C. A. *J. geophys. Res.* **78,** 470–475 (1973).
7. Bender, P. L. & Goad, C. in *The Use of Artificial Satellites for Geodesy and Geodynamics 2*, 145–171 (eds Veis, G. & Livieratos, E.) (National Technical University, Athens 1979).
8. Gaposchkin, E. M. *Adv. Space Res.* **1,** (1981).
9. Morrison, L. V. & Stephenson, F. R. in *Sun and Planetary System* (eds Fricke, W. & Teleki, G.) (Reidel, Boston 1982).
10. O'Connell, R. J. *Geophys. J. R. astr. Soc.* **23,** 299–327 (1971).
11. Peltier, W. R. & Wu, P. *Geophys. Res. Lett.* **10,** 181–184 (1983).
12. Smith, D. E. & Dunn, P. J. *Geophys. Res. Lett.* **7,** 437–440 (1980).
13. Munk, W. H. & MacDonald, G. J. F. *The Rotation of the Earth* (Cambridge University Press, New York, 1975).
14. Lambeck, K. *The Earth's Variable Rotation* (Cambridge University Press, New York, 1980).
15. Yoder, C. F., Williams, J. G. & Parke, M. E. *J. geophys. Res.* **86** (B2), 881–891 (1981).
16. Van Hycklama, T. E. A. in *Proc. Reading Symp. World Water Balance, Publ.* 92 (AIHS–UNESCO, 1970).
17. Nakiboglu, S. M. & Lambeck, K. *Geophys. J.R. astr. Soc.* **62,** 49–58 (1980).
18. Sabadini, R. & Peltier, W. R. *Geophys. J.R. astr. Soc.* **66,** 533–578 (1981).
19. Gornitz, V., Lebedev, S. & Hansen, J. *Science* **215,** 1611–1614 (1982).
20. Hide, R., Birch, N. T., Morrison, L. V., Shea, D. J. & White, A. A. *Nature*, **286,** 114–117 (1980).
21. Braginsky, S. I. & Fishman, V. M *Geomag Aeron.* **18,** 225–231 (1978).
22. Rochester, M. G. & Smylie, D. E. *J. Geophys. Res.* **79,** 4948–4954 (1974).
23. Fliegel, H., Dickey, J. O. & Williams, J. G. in *High-Precision Earth Rotation and Earth–Moon Dynamics*, 53–88 (ed. Calame, O.) (Reidel, Boston 1982).
24. *Annual Report for 1981*, (Bureau International de l'Heure, Paris, 1982).
25. Proudman, J. *Geophys. J.R. astr. Soc.* **3,** 244–289 (1960).
26. Lisitzin, E. *Sea Level Changes* (Elsevier, Amsterdam 1974).
27. Rossiter, J. R. *Geophys. J.R. astr. Soc.* **12,** 259–299 (1967).
28. Currie, R. G. *Geophys. J.R. astr. Soc.* **46,** 513–520 (1976).
29. Morrison, L. V. in *Tidal Frictional Earth's Rotation* (eds Brosche, P. & Sündermann, J.) (Springer, Berlin, 1978).
30. Dickey, J. O., Newhall, X X, Williams, J. G. & Yoder, C. F. *EOS* **64,** 204 (1983).
31. Wu, P. & Peltier, W. R. *Geophys. J.R. astr. Soc.* (in the press).
32. Clark, J. A. & Lingle, C. S. *Quat. Res.* **11,** 279–298 (1979).
33. Hughes, T. *et al.* in *The Last Great Ice Sheets* (eds Denton, G. H. & Hughes, T.) (Wiley, New York, 1981).
34. Peltier, W. R. in *Physics of the Earth's Interior* (eds Dziewonski, A. & Boschi, E.) (Elsevier, New York 1980).
35. Balmino, G., Lambeck, K. & Kaula, W. M. *J. geophys. Res.* **78,** 478–481 (1975).
36. Rubincam, P. D. *Celest. Mech.* **26,** 361–382 (1982).
37. Rubincam, P. D. *Nasa Mem.* 84982 (1983).

Constraints on evolution of Earth's mantle from rare gas systematics

Claude J. Allègre, Thomas Staudacher, Philippe Sarda & Mark Kurz

Laboratorie de Geochimie et Cosmochimie, Institut de Physique du Globe et Département des Sciences de la Terre, 4 Place Jussieu, 75230 Paris Cedex 05, France

Analyses of the isotopic composition of He, Ar and Xe in a suite of glasses from the mid-ocean ridges and from the island of Hawaii show that the Hawaiian samples have systematically lower $^4He/^3He$, $^{40}Ar/^{36}Ar$ and $^{129}Xe/^{130}Xe$ ratios than the mid-ocean ridge basalts. We interpret this result to imply the existence of an undegassed mantle reservoir. Given the isotopic variations, and the half lives of ^{129}I and ^{40}K (parent isotopes of ^{129}Xe and ^{40}Ar), the undegassed reservoir must have been separated from the MORB source reservoir at least 4,400 Myr ago. The most reasonable explanation for the data is therefore the existence of a two-layered mantle.

THE search for the driving mechanism of plate tectonics has led geophysicists to propose a series of convective mantle models. Morgan[1] proposed the existence of a separate deep mantle, which would generate plumes. McKenzie and Richter[2] proposed a two-layer convection mantle, with a boundary layer at 700 km (maximum depth of earthquakes). On the other hand, several authors[3–5] have argued that geophysical evidence favours whole-mantle convection.

Measurements of isotope ratios in mantle-derived basalts have shown that the mantle is heterogeneous. Based on Sr and Nd isotopic information alone, early studies showed that distinction could be made between a depleted mantle source (that is, the source of mid-ocean ridge basalts (MORB)), and an undepleted mantle, from which oceanic island basalts are derived (see reviews in ref. 6). Assuming that depletion is caused by the extraction of continental crust, and using the geochemical budgets for Sr and Nd, several authors[7–10] calculated that the depleted mantle represents one-third or half of the whole mantle.

Reconciling this conclusion with a two-layered mantle model, these authors assume that the upper 700 km correspond to the depleted mantle. There are several major criticisms of this model. First, it is not clear that depletion is created only by extraction of continental crust, since basaltic extraction on the ridge crest may also have an important role[7,11]. Second, the geochemical budget calculations do not yield the relative geometry of the two assumed mantle reservoirs. Finally, the assumption of only two geochemically homogeneous distinct reservoirs is an oversimplification[10,12,13].

Nd–Sr isotope geochemistry does not allow a unique choice to be made between whole-mantle and layered-mantle convection. For example, proponents of whole-mantle convection have argued that the geochemical heterogeneities can be explained by a lumpy mantle, rather than a layered one (see ref. 14). This would require that the lumps maintain their identity over long periods of time, and are entrained in the overall circulation pattern.

We now report new noble gas measurements on oceanic basalt glasses, and illustrate the importance of these data to the above arguments. Although in recent years several noble gas studies have been carried out on mantle derived rocks (see refs 12, 15–21) this information has not received the attention that it deserves. The noble gases can yield unique constraints on the structure and evolution at the mantle for several reasons.
(1) Due to the volatility of the noble gases, and the involatility of the radioactive parent isotopes (^{40}K, ^{238}U, ^{235}U, ^{232}Th, ^{244}Pu), the isotope evolution is strongly affected by degassing, which is not the case for the Sm–Nd and Rb–Sr systems. Therefore, the variation of mantle noble gas isotope ratios depends on the degassing history of the mantle, and are a function of continental extraction processes only through their parent isotopes.
(2) The radioactive parent isotopes decay with very different half lives which provides unique temporal information. The extinct isotopes ^{129}I and ^{244}Pu had very fast decay constants

0028–0836/83/260762—05$01.00